



Optimization of Air Electrode for Li/Air Batteries

Jie Xiao,^{*} Donghai Wang,^{a,*} Wu Xu,^{*} Deyu Wang,^{**} Ralph E. Williford,
Jun Liu, and Ji-Guang Zhang^{*,z}

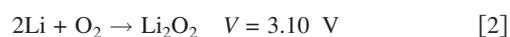
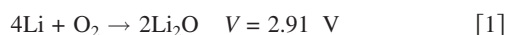
Energy and Environment Directorate, Pacific Northwest National Laboratory, Richland,
Washington 99354, USA

The effects of carbon microstructure and loading on the performance of Li/air batteries were investigated. We found that the capacities of Li/air batteries were related to both the specific capacity per unit weight of the carbon source (mAh g^{-1}) and the carbon loading per unit area (g cm^{-2}). Therefore, the product of these two parameters [i.e., the area-specific capacity (mAh cm^{-2})] was introduced to optimize the performance of the air electrode. At the fixed electrolyte amount ($100 \mu\text{L}/\text{cell}$), the best area-specific capacity of 13.1 mAh cm^{-2} was obtained at a carbon loading of 15.1 mg cm^{-2} . Further increase or decrease in the carbon loading led to a reduced area-specific capacity. The capacities of air electrodes increased with increasing mesopore volumes of the carbon sources. The uniformity of the pore sizes also played an important role in determining the electrochemical performances of the Li/air batteries. At fixed carbon loading and discharge rates, the capacity increased significantly with increasing electrolyte amounts. This phenomenon was explained by the formation of extra triphase regions in the air electrodes. After optimizing the electrode and electrolyte parameters, a high capacity of 1756 mAh g^{-1} carbon was obtained for Li/air batteries operated in ambient oxygen pressure (0.21 atm).

© 2010 The Electrochemical Society. [DOI: 10.1149/1.3314375] All rights reserved.

Manuscript submitted October 9, 2009; revised manuscript received December 9, 2009. Published March 3, 2010.

Traditional cathode materials used in Li-ion batteries, such as LiCoO_2 and LiFePO_4 , have limited capacities ranging from 130 to 150 mAh g^{-1} because of the nature of their crystalline structure and their electrochemical properties. Charge storage in Li-ion batteries is insufficient to satisfy the ever-increasing requirements for batteries with both high capacities and high energy densities. Recently, Li/air batteries have attracted interest because they exhibit significant advantages over conventional energy-storage devices.¹⁻¹¹ Among all practical electrochemical couples, Li/air has the largest theoretical specific energy ($11,972 \text{ Wh kg}^{-1}$). In a Li/air battery, the cathode material, oxygen, is absorbed directly from the environment during the discharge process. The electrochemical reactions involved in this process can be described as Eq. 1 and 2



A Li/air battery using an organic electrolyte was first reported by Abraham and Jiang.¹ Based on a polymer electrolyte and a 0.3 mm thick air electrode, a specific capacity of 1600 mAh g^{-1} carbon was obtained. They also reported that the specific capacity of Li/air batteries decreased with decreasing surface area of the carbon sources. The performance of Li/air batteries is also influenced by several other factors, including carbon source, carbon loading,¹ oxygen partial pressure,² and electrolyte selection.^{2,3,9} These factors are directly related to the oxygen diffusion process in the air electrode. Although several groups have reported high specific capacity of air electrodes, most of these results^{5,8,10,11} were obtained in a pure oxygen environment, where oxygen partial pressure is larger than 1 atm. An investigation of Li/air batteries in this environment is convenient for fundamental studies and has already established a good understanding of this system.^{2,6,8-11} However, to fully realize the potential of Li/air batteries, they need to be operated in ambient conditions (where oxygen partial pressure is only 0.21 atm). Read et al.² reported that the capacity of Li/oxygen batteries at 0.21 atm was only about one-fifth of those obtained in a pure oxygen environment in which the oxygen pressure is larger than 1 atm. Therefore, it is critical to further investigate the performance of Li/air batteries in more practical conditions (with an oxygen partial pressure of 0.21 atm).

The structure of carbon used in the air electrode is another critical factor that affects the performance of Li/air batteries. Zhang et al.¹¹ indicated that the real capacity of a Li/air battery did not correspond to the theoretical capacity of metallic lithium, resulting from the insolubility of discharge products (Li_2O_2 and Li_2O) in nonaqueous organic electrolytes. Instead, the real capacity that a Li/air battery can achieve is determined by the carbon air electrode, especially with respect to the pore volume available for the deposition of discharge products, rather than the lithium anode. This is the primary reason that most works in Li/air battery research have reported the performance of a battery in terms of carbon weight (i.e., mAh g^{-1} carbon). For the practical application of Li/air batteries, it is critical to choose a carbon source with a good catalytic surface and microstructure to facilitate a Li/ O_2 reaction and to hold a maximum amount of reaction products (which is proportional to the battery capacity) per gram of carbon.

Once a good carbon source is identified, it is also important to increase the carbon loading (mg cm^{-2}) in the air electrode to maximize the capacity of both the air electrode and the Li/air battery. This is because the capacity of a Li/air battery is directly proportional to its surface area. Several groups have reported good capacity per gram of carbon;^{8,10} however, a very low carbon loading (ca. 2 mg/cm^{-2}) was used to reach this high capacity ($>4000 \text{ mAh g}^{-1}$ carbon). When carbon loading is increased to more than 7 mg/cm^{-2} , the specific capacity of batteries quickly dropped to less than 300 mAh g^{-1} carbon. Therefore, when we move from the optimization of carbon to the optimization of the complete Li/air batteries, both the carbon source and the carbon loading must be optimized.

In this work, different carbon sources were investigated for their application in Li/air batteries operated in dry air environment. A more practical parameter, the area-specific capacity (mAh cm^{-2}) of the air electrode, was used to optimize the structure of the air electrode, especially carbon loading on the performance of Li/air batteries. The effects of several other parameters that affect the performance of Li/air batteries were investigated as well.

Experimental

Preparation and selection of carbon sources.—Several commercial carbon materials, such as BP2000 (Cabot Corp.), Calgon (Calgon Carbon Corp.), Denka (Denka Corp., Japan), and Ketjen black (KB) EC600JD (Akzo Nobel Corp.) were investigated. Ball-milled KB was also prepared and evaluated. These commercial carbon sources have a wide distribution of mesopore sizes. In an effort to further improve the performance of Li/air batteries, mesopore carbons with a narrow distribution of mesopore sizes were prepared

* Electrochemical Society Active Member.

** Electrochemical Society Student Member.

^a Present address: The Pennsylvania State University, Department of Mechanical and Nuclear Engineering, University Park, PA 16802, USA.

^z E-mail: jiguang.zhang@pnl.gov

using a surfactant-templated, self-assembly process.¹² In this process, 0.30 g phenol, 0.06 g NaOH (20%), and 0.53 g formalin (37%) were reacted at 70°C for 1 h. After neutralization to pH 7 using HCl solution, the water in the solution was removed under vacuum. The obtained phenol oligomer (0.5 g) and 0.25 g triblock copolymer Pluronic F127 [(EO)₁₀₆(PO)₇₀(EO)₁₀₆, where EO and PO are ethylene oxide and propylene oxide, respectively] were individually dispersed in 5.0 g of ethanol by sonication. Afterward, they were mixed together and kept in sonication. The solution was placed in Petri dishes overnight to evaporate ethanol at room temperature and then heated in an oven at 100°C for 24 h. The as-prepared products, transparent flexible yellow films, were scraped from the dishes followed by calcination under an inert atmosphere (Ar/3% H₂) with a flow rate of 90 cm³/min at 900°C for 3 h to obtain mesoporous carbon (denoted as JMC).

Preparation of carbon mix.— The mixing process of carbon (especially KB carbon) required special attention during electrode preparation. Unlike common carbon sources such as Calgon, BP2000, or acetylene black, it is very difficult to roll the highly porous KB into a whole sheet. Thus, a special procedure has been developed to prepare the KB-based air electrode, as described below.

KB was first immersed in distilled water for 20 min and then mixed with DuPont Teflon PTFE-TE3859 fluoropolymer resin aqueous dispersion (60 wt % solids). The weight ratio of KB and Teflon after drying was 85:15. The mixture was then laminated into a continuous carbon sheet using a roller calendar with adjustable pressures ranging from 0 to 100 psi. A nickel mesh was laminated onto the carbon sheet to serve as the current collector. To minimize moisture penetration, a porous Teflon film (3 μm thick, W. L. Gore and Associates, Inc.) was also laminated on one side of the electrode, which was exposed to air during cell operation. Circular disks (1.98 cm²) with 2 × 2 mm nickel tabs on their edges were punched from the air electrode and used in cell assembly.

Characterization.— The structure of different types of carbons was characterized by using a Philips X'Pert X-ray diffractometer in a θ-2θ scan mode and Cu Kα radiation at λ = 1.54 Å. All samples were scanned at 1.8°/min between different ranges. N₂ adsorption/desorption data were collected using a Quantachrome Autosorb automated gas sorption system. The surface area of the carbon materials was analyzed by the Brunauer, Emmett, and Teller (BET) method. The total pore volume and pore size distribution were evaluated by the Barrett–Joyner–Halenda (BJH) method. The morphologies of the electrodes were examined using a scanning electronic microscope (SEM, JSM 5900 LV, JEOL) with a maximum resolution of 30 Å.

Li/air coin cells were assembled in an argon-filled glove box (MBraun Inc.) in which the moisture and oxygen concentration were both less than 1 ppm. Type 2325 coin cell kits (Canadian National Research Council, Canada) were used to fabricate test devices. The cell had a diameter of 23 mm and a thickness of 2.5 mm. The positive pans of the coin cells were drilled with 19 ∅ 1.0 mm holes, which were evenly distributed on the cell pans to allow air to ingress (see Fig. 1). The small tab on the circular electrode was spot welded onto the positive pan to create a stable electrical contact. A lithium disk (1.59 cm in diameter and 0.5 mm thick) was used as the anode. The electrolyte was optimized⁹ and prepared by dissolving 1 mol lithium bis(trifluoromethanesulfonyl)imide (battery grade, Ferro) in ethylene carbonate/propylene carbonate (1:1 weight ratio). The salts and solvents used in the electrolyte were all battery-grade materials purchased from Ferro Corporation. A Whatman GF/D glass microfiber filter paper (1.9 cm in diameter) was used as the separator because of its ability to hold more electrolyte than other separators. Unless specified otherwise, 100 μL of electrolyte was added to each of the cells. The electrochemical tests of Li/air coin cells were performed in dry air at room temperature using an Arbin BT-2000 battery tester. The coin cells were placed in a glove box filled with

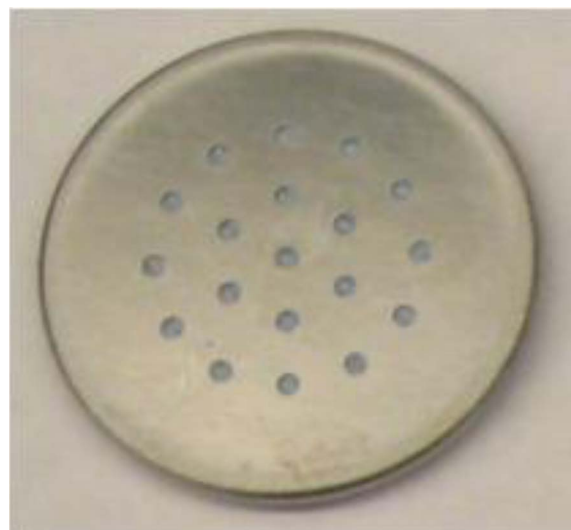


Figure 1. (Color online) Picture of a Li/air cell (type 2325) with multiple air diffusion holes.

dry air to minimize the influence of moisture. The glove box contained a gas inlet and outlet to maintain a positive pressure inside by allowing dry air to continuously flow through. The humidity inside the glove box was less than 1% relative humidity and was measured by a Dickson handheld temperature/humidity/dew point monitor. The cells were discharged at a constant current density (*I*) to 2.0 V and then held at 2.0 V until the discharge current density decreased to less than *I*/5. Unless specified otherwise, the discharge current density was 0.05 mA cm⁻². To compare with previously published literature, both the specific capacity per carbon weight and the area-specific capacity of the electrode are reported in this paper.

Results and Discussion

The nanostructure of carbon sources plays an important role in the performance of Li/air batteries. Several works have reported that the specific energy of Li/air batteries increased with increasing mesopore volume of carbon sources used in their air electrode. The effects of pore size distribution and pore volume of several carbon sources were further investigated in this work. Figure 2 shows the BJH pore size distribution of several carbon materials investigated in this work. JMC carbon has a very narrow distribution of pore diameters centered at 3.5 nm, as shown in Fig. 2a. Commercial carbon materials including Calgon, Denka, and BP2000 have mesoporous structures with broad pore size distribution, as shown in Fig. 2b-d. Figure 2e shows the BJH pore size distribution of KB, which has a pore size distribution peaked at ~3 nm, but it also has a significant amount of pores with much larger sizes. Figure 2f shows the pore size distribution of KB after ballmilling for 30 min. No peak in the pore size distribution curves of KB was observed after it was ballmilled. In contrast, JMC has a uniform pore size distribution but relatively low pore volume. KB has both relatively uniform pore size (3–10 nm) and high pore volume, whereas the other commercial carbon materials show less uniform pore size and low pore volume.

The physical properties including microstructure, surface area, pore size, and pore volume of the carbon materials are summarized in Table I. Calgon carbon consists of crystalline graphite, whereas BP2000, Denka, and KB exhibit poor crystalline graphite. However, KB became amorphous after 30 min ballmilling. The as-prepared JMC exhibits an ordered mesoporous structure in an amorphous state, as revealed by the low angle X-ray diffraction (XRD) pattern.^{12,13} KB has the highest measured total pore volume (7.651 cm³/g). However, after 30 min of ballmilling, the pore volume of KB decreases dramatically to only 0.4334 cm³ g⁻¹. A significantly reduced BET surface area (from 2672 to 342.4 m² g⁻¹) is

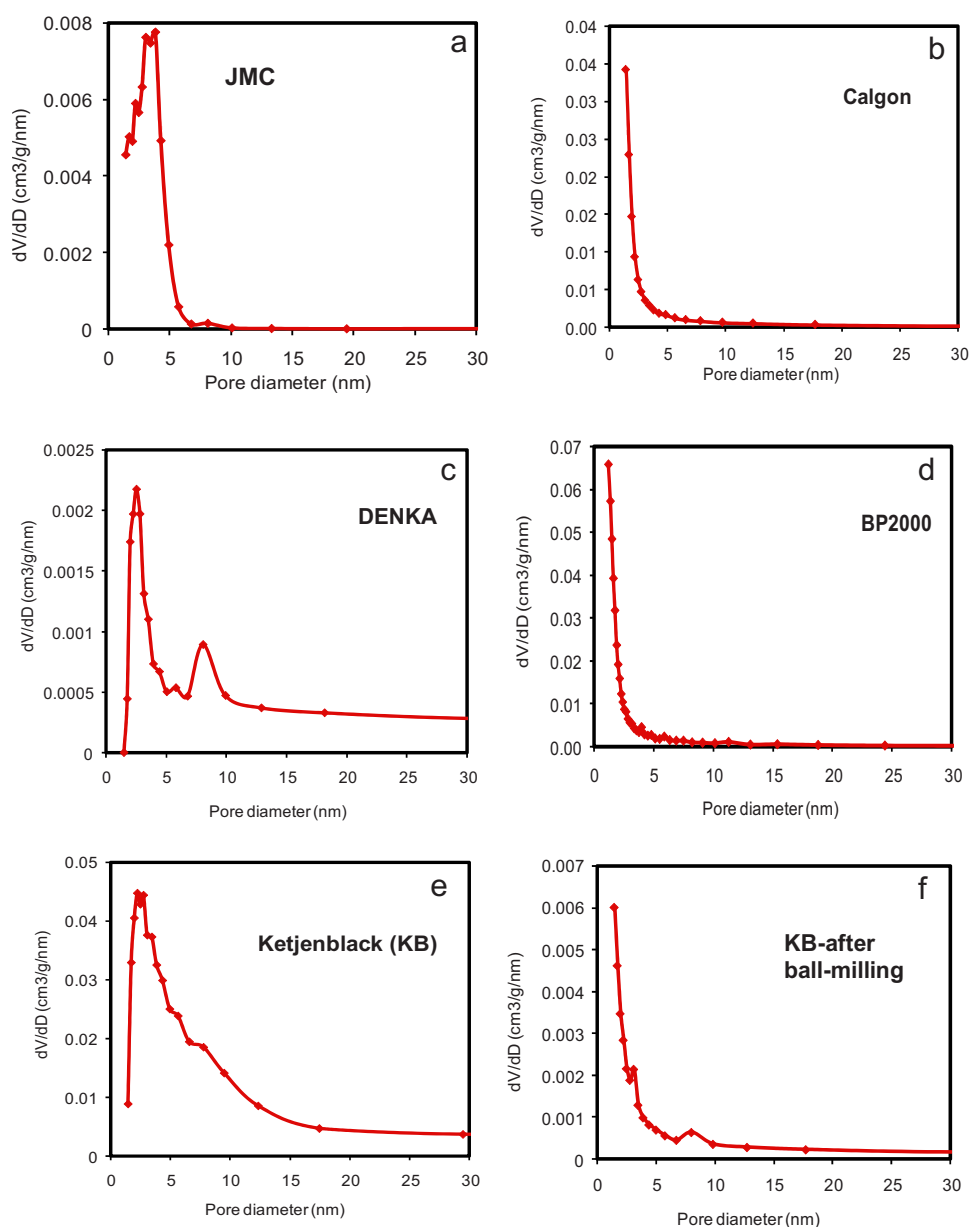


Figure 2. (Color online) Pore size distribution of various carbons investigated in this work: (a) JMC carbon prepared by self-assembly method, (b) Calgon carbon, (c) Denka carbon, (d) BP2000 carbon, (e) KB carbon (as received), and (f) KB after ballmilling for 30 min.

also observed for the ballmilled KB. The other commercial carbons exhibited relatively small pore volumes ($<1 \text{ cm}^3/\text{g}$).

The discharge capacities of Li/air batteries based on different carbon sources are compared in Fig. 3. The specific capacity (mAh g^{-1} carbon) for each cell has the following order from high to low: $\text{KB} > \text{Calgon} > \text{ballmilled KB} \approx \text{BP2000} > \text{JMC} > \text{Denka}$. The excellent performance of KB-based Li/air batteries can be attributed to its high mesopore volume. After ballmilling, the

pore volume ($0.4334 \text{ cm}^3/\text{g}$), specific capacity (47 mAh g^{-1}), and surface area ($342.4 \text{ m}^2 \text{ g}^{-1}$) of KB were reduced to 5.6, 5.5, and 12.8% of their original values, respectively. This result clearly indicates a direct correlation between the mesopore volume of carbon and the specific capacity of Li/air batteries, especially when there is a large difference in pore volume between the carbon sources. We also found that although Denka black carbon has a larger pore volume ($0.5355 \text{ cm}^3 \text{ g}^{-1}$) than that of JMC carbon ($0.2376 \text{ cm}^3 \text{ g}^{-1}$),

Table I. Surface area and pore volume comparison.

| | Surface area ($\text{m}^2 \text{ g}^{-1}$) | Pore volume ($\text{cm}^3 \text{ g}^{-1}$) | BJH pore size (nm) | Microstructure from XRD |
|---------------|---|---|------------------------------------|----------------------------------|
| KB | 2672 | 7.6510 | 2.217–15 nm | Poor crystalline graphite |
| Ballmilled KB | 342.4 | 0.4334 | No clear peak in size distribution | Amorphous |
| BP2000 | 1567 | 0.8350 | No clear peak in size distribution | Poor crystalline graphite |
| Calgon | 1006 | 0.5460 | No clear peak in size distribution | Crystalline graphite |
| Denka black | 102.0 | 0.5355 | 2.511 and 6 nm | Poor crystalline graphite |
| JMC | 548.7 | 0.2376 | 3–3.8 nm | Amorphous with ordered mesopores |

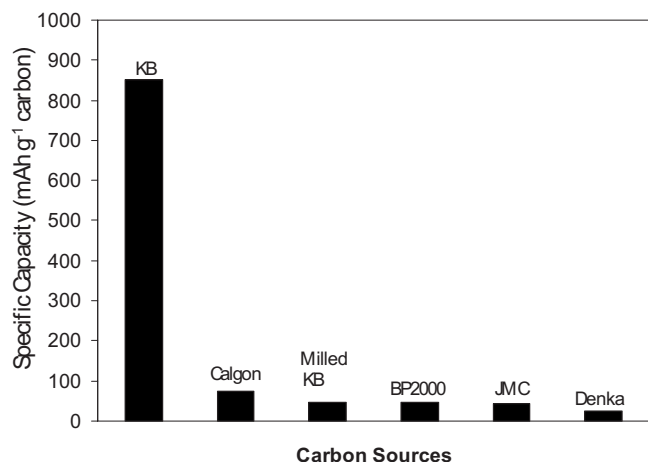


Figure 3. Comparison of the discharge capacities Li/air batteries using different carbons. All the coin cells are discharged to 2.0 V at 0.05 mA cm^{-2} and then held at 2.0 V until I' is less than $I/5 = 0.01 \text{ mA cm}^{-2}$.

the Li/air batteries using Denka carbon-based air electrode exhibit a capacity much smaller than that using JMC carbon-based air electrode, as shown in Fig. 3. It is expected that both too large and too small pore sizes lead to a less efficient use of mesopore volumes. Therefore, JMC carbon (which has a narrow distribution of mesopore size centered on $\sim 3.5 \text{ nm}$) could be used more efficiently than Denka black carbon (which has a wide distribution of pore sizes).

The specific capacity of Li/air electrode strongly depends on the porosity of the electrode. The KB-based electrode was prepared by a dry rolling method in this work. Because KB is a highly porous material with a chainlike structure, the thickness of the electrode can expand after it was compressed under higher pressure. Therefore, no significant change in its porosity was observed for the electrode prepared under different loadings and pressures. [A constant ratio of KB: poly(tetrafluoroethylene) (PTFE) (85:15) was used in this work.] The porosity of the KB-based electrode is mainly determined by its mesopore volume and highly springlike structure, especially after it was soaked with an electrolyte, as discussed later.

As shown in Fig. 3, KB-based air electrodes exhibit the highest specific capacity (851 mAh g^{-1} at 0.05 mA cm^{-2}). This value is not as high as some of the best results reported before. The main reasons for this difference can be attributed to the more practical test conditions and cell configuration used in this work. One is that all of the cells in this work were tested in a practical oxygen partial pressure (0.21 atm), which is much lower than those used in most of the previous works ($> 1 \text{ atm}$). The specific capacity of the cells tested at 0.21 atm was only about one-fifth of those tested at higher pressures ($> 1 \text{ atm}$), as indicated by Read et al.² Another reason is that the carbon loading used in this work was higher than those of previous works. Most of the previous works have used the mAh g^{-1} carbon when reporting the performance of Li/air batteries. Although this value may increase with decreasing carbon loading, too small a carbon loading per unit area leads to a small capacity per unit area of a practical Li/air battery. Considering the fact that the capacity of a Li/air battery is always proportional to the area of the air electrode exposed to air, the capacity of the Li/air cells is proportional to both the specific capacity per gram carbon (mAh g^{-1}) and carbon loading per unit area (g cm^{-2}); the product of these two parameters [i.e., the area-specific capacity (mAh cm^{-2})] was introduced in this work as a more practical parameter to optimize the performance of the complete air electrode used in practical Li/air cells.

To further illustrate this idea, we compare the plots of both specific capacity (mAh g^{-1} carbon) and area-specific capacity (mAh cm^{-2}) of Li/air cells as a function of carbon loading (mg cm^{-2}), as shown in Fig. 4. Although the specific capacity of the

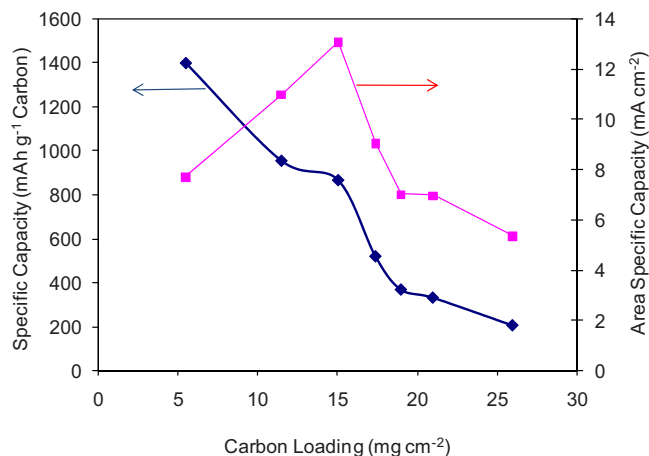


Figure 4. (Color online) Relationship between capacity and carbon loading. The left axis shows the specific capacity (mAh g^{-1} carbon) of the air electrode; the right axis shows the area-specific capacity (mAh cm^{-2}) of the same air electrode. All cells are discharged to 2.0 V at 0.05 mA cm^{-2} and then held at 2.0 V until the current density is less than or equal to 0.01 mA cm^{-2} in a dry air environment.

cells decreases monotonically with increasing carbon loading, a maximum area-specific capacity of 13.1 mAh cm^{-2} is found at a carbon loading of 15.1 mg cm^{-2} . When the carbon loading is less than 15.1 mg cm^{-2} , although a higher specific capacity (mAh g^{-1} carbon) can be obtained, the capacity per unit area of the Li/air cell decreases because less active material per unit area is used. When the carbon loading exceeds 15.1 mg cm^{-2} , the area-specific capacity of Li/air cell also decreases because a thicker electrode leads to a lower utilization of the active carbon.

The specific capacity data shown in Fig. 4 are higher than those reported by another group⁸ when the same carbon loadings are compared. There are several reasons for this improvement. First, the optimized carbon loading and preparation conditions during electrode fabrication provide better electrode porosity suitable for lithium/oxygen reaction. Second, the optimized electrolyte used in this work is relatively stable in air, and it has a low wettability when contacted with the air electrode.⁹ The highly hydrophobic PTFE binder used in this work may also lead to higher oxygen flow rates than the poly(vinylidene fluoride) binders used in another work.⁸

Microstructures and morphologies of the air electrode have been investigated. Figure 5 shows SEM micrographs of the electrode material before rolling into an electrode sheet (see Fig. 5a and b), after the rolling process (see Fig. 5c and d), and after discharge (see Fig. 5e and f). No apparent changes in the porosity of the electrode material before and after the rolling process are observed. However, a comparison of the images in Fig. 5d and f indicates that the porosity of the electrode decreases significantly after discharge. The reduced porosity can be attributed to the occupation of pores by the reaction product (Li_2O or Li_2O_2).

Based on the optimized carbon loading (15.1 mg cm^{-2}) and the electrode thickness, the influence of current density on the air electrode is investigated. Figure 6 shows the typical discharge curves for a Li/air battery using KB as the cathode carbon material at different discharge rates. The discharge capacity shows a rapid decrease from 851 mAh g^{-1} at 0.05 mA cm^{-2} to 432 mAh g^{-1} at 0.1 mA cm^{-2} . In addition, the increased discharge current also lowers the discharge plateau because of the increased polarization. The capacity loss at a high discharge rate can be attributed to the quick deposition of $\text{Li}_2\text{O}_2/\text{Li}_2\text{O}$ on the surface of the air electrode, which limits oxygen access to the inner layer of the carbon electrode and incomplete utilization of the carbon electrode.

After being discharged to 2.0 V, the cell voltage is held at 2.0 V until the current density becomes less than $I/5$ ($I = 0.05, 0.1$, or

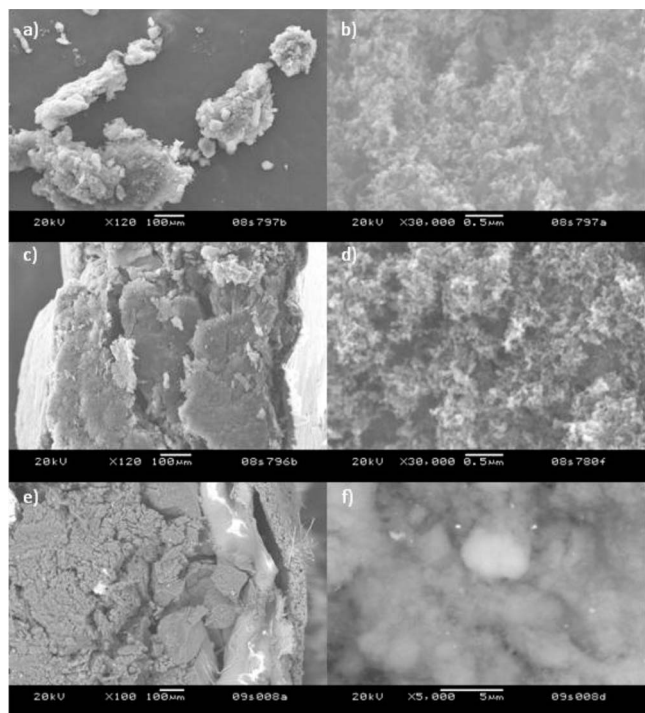


Figure 5. SEM micrograph of air electrodes: (a) KB + PTFE powder before rolling (low magnification), (b) KB + PTFE powder before rolling (high magnification), (c) KB + PTFE powder after rolling (low magnification), (d) KB + PTFE powder after rolling (high magnification), and (e) KB + PTFE electrode material after discharge (low magnification). The PTFE membrane is shown on the right; (f) KB + PTFE electrode material after discharge (high magnification).

0.2 mA cm⁻²). At a low current density of 0.05 mA cm⁻², the surface of the air electrode is not fully blocked when reaching the constant voltage step. Thus, a small amount of oxygen can still diffuse to the electrode and react with lithium. At 0.05 mA cm⁻², the capacity from this constant voltage plateau (see Fig. 6) contributed 228 mAh g⁻¹, which is 26.3% of the total capacity. However, when the discharge rate increases to 0.2 mA/cm², the capacity from the constant 2.0 V step is reduced to only 13 mAh g⁻¹. This is consistent with the nearly complete blocking of the air electrode at a high current density.

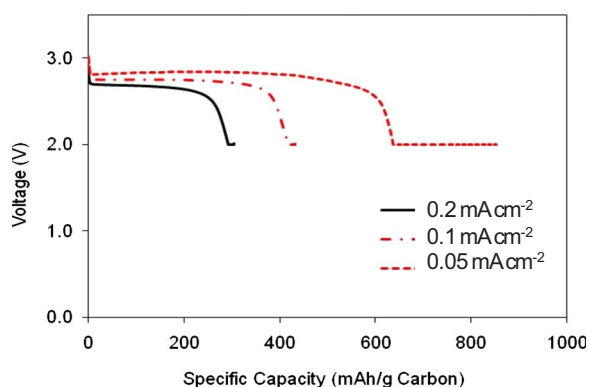


Figure 6. (Color online) Discharge curves of Li/air coin cells at different current densities. Carbon loading is 15.1 mg cm⁻² for all the tests. The cells are discharged to 2.0 V at 0.05, 0.1, and 0.2 mA cm⁻² and held at 2.0 V until the current becomes less than 1/5. The electrolyte amount in all the coin cells was 100 μ L.

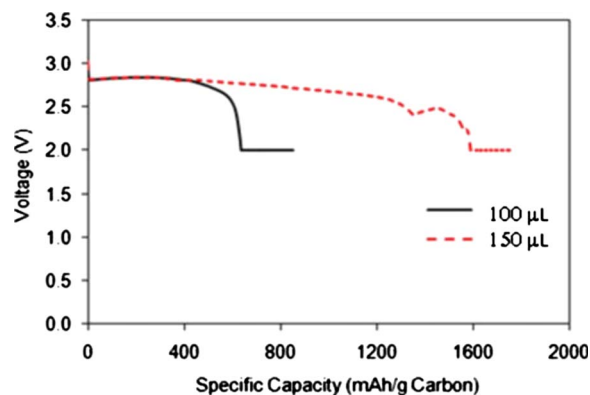


Figure 7. (Color online) Comparison of the discharge curves for Li/air coin cells containing 100 and 150 μ L of electrolyte. The carbon loading is 15.1 mg cm⁻². The cell is discharged to 2.0 V at $I = 0.05$ mA cm⁻² and held at 2.0 V; the current becomes less than 0.01 mA cm⁻².

The carbon loading and current density have significant effects on oxygen diffusion in the air electrode and performance of Li/air batteries, as discussed above. The electrolyte, however, also plays an important role on the transport of the dissolved oxygen and battery performance. The effects of different electrolytes on the performance of Li/air batteries have been recently reported by Xu et al.⁹ In this work, we further investigate the effect of electrolyte volume on the KB-based Li/air battery. In the experiments discussed above, 100 μ L of the electrolyte was used in the coin cells. However, we found that the discharge capacity of Li/air batteries increased from 851 mAh g⁻¹ carbon to 1756 mAh g⁻¹ carbon when the amount of electrolyte was increased from 100 to 150 μ L. Figure 7 shows a comparison of the specific capacity of Li/air batteries with different amounts of electrolyte. The spike in the voltage profile of the sample using 150 μ L electrolyte came from a power outage during a long-term discharge process. This high specific capacity corresponds to a specific energy of 4614 Wh kg⁻¹. The significant increase in the cell capacity with increasing amounts of electrolyte can be attributed to a large volume expansion of the KB-based air electrode after they were soaked with electrolyte. KB carbon exhibits a chainlike structure and has a much larger mesopore volume than most other carbon sources. When the electrolyte was added to the air electrode, the chain structures in Ketjen black expanded like a spring, thus exposing more porous structures. Subsequently, more electrolytes were required to wet the freshly generated carbon surfaces/pores. The porosity of the air electrode increases after being soaked in the electrolyte. This process forms more triphase regions, which facilitates the Li/O₂ reaction and holds more reaction products. Consequently, the cell capacity was significantly improved. The volume-change and pore-generation processes in KB are shown in Fig. 8. We observed that the thickness of a KB-based air electrode increased more than 100% (from 0.71 to 1.57 mm) after it was soaked in the electrolyte overnight, but the thickness of the air electrode based on other carbons does not change significantly. Because all the air electrodes investigated in this work used the same weight ratio of carbon to binder (85:15), the swelling of the KB-based air electrode can be mainly attributed to KB carbon itself. For the type 2325 coin cell kits used in this work, 150 μ L is the maximum amount of electrolytes that could be absorbed without any leakage in the cells with multiple diffusion holes, as shown in Fig. 1.

Conclusions

Various carbon sources were investigated for their application in air electrodes of Li/air batteries. Ketjen black carbon, which has the highest mesopore volume among all of the carbon sources tested in this work, demonstrated the highest specific capacity when operated in a dry air environment where the oxygen partial pressure is 0.21 atm. After soaking in the electrolyte, the KB-based electrode ex-

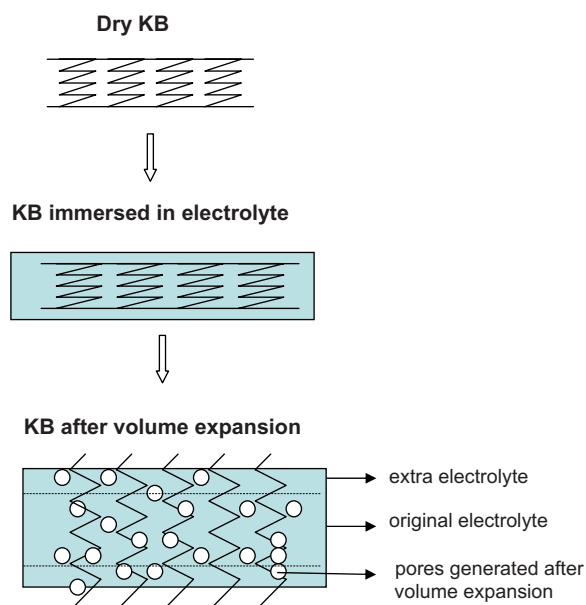


Figure 8. (Color online) Symbolic drawing on the pore-formation process of a KB-based air electrode.

panded significantly ($> 100\%$) and absorbed much more electrolyte than electrodes made of other types of carbons. The large volume expansion in the KB-based electrode led to extra triphase regions to facilitate the Li/O_2 reaction in the electrode and extra volume to hold the reaction product ($\text{Li}_2\text{O}/\text{Li}_2\text{O}_2$). Consequently, the Li/air cells using KB-based air electrode exhibited the highest specific capacity among all samples. To further improve the performance of complete Li/air batteries, a more practical criterion, the area-specific capacity (mAh cm^{-2}), was introduced to optimize the air electrode. At a fixed electrolyte amount ($100 \mu\text{L}/\text{cell}$), the best area-specific capacity of 13.1 mAh cm^{-2} was obtained at a carbon loading of

15.1 mg cm^{-2} , where the optimal balance between the mass loading and the utilization rate of carbon was reached. After optimizing the electrode porosity/thickness and electrolyte amount, a high capacity of 1756 mAh g^{-1} carbon corresponding to an area-specific capacity of 26.5 mAh cm^{-2} was obtained for Li/air batteries operated in a dry air environment.

Acknowledgments

This work was supported by the U.S. Defense Advanced Research Projects Agency. Funding from the Laboratory Directed Research and Development Program at Pacific Northwest National Laboratory (PNNL) supported the preparation of this paper. The authors thank Zimin Nie of PNNL for her help with the XRD characterization of the samples and Dr. Gordon L. Graff of PNNL for the useful suggestions on the manuscript. This paper has been approved for public release with unlimited distribution.

Pacific Northwest National Laboratory assisted in meeting the publication costs of this article.

References

1. K. M. Abraham and Z. Jiang, *J. Electrochem. Soc.*, **143**, 1 (1996).
2. J. Read, K. Mutolo, M. Ervin, W. Behl, J. Wolfenstine, A. Driedger, and D. Foster, *J. Electrochem. Soc.*, **150**, A1351 (2003).
3. T. Kuboki, T. Okuyama, T. Ohsaki, and N. Takami, *J. Power Sources*, **146**, 766 (2005).
4. J. Read, *J. Electrochem. Soc.*, **149**, A1190 (2002).
5. A. Doble, C. Morein, and K. Abraham, Abstract 823, The Electrochemical Society Extended Abstracts, Vol. 2005-2, Los Angeles, CA, Oct 16–21, 2005.
6. T. Ogasawara, A. Débart, M. Holzapfel, P. Novák, and P. G. Bruce, *J. Am. Chem. Soc.*, **128**, 1390 (2006).
7. A. Débart, A. J. Paterson, J. Bao, and P. G. Bruce, *Angew. Chem., Int. Ed.*, **47**, 4521 (2008).
8. S. D. Beattie, D. M. Manolescu, and S. L. Blair, *J. Electrochem. Soc.*, **156**, A44 (2009).
9. W. Xu, J. Xiao, J. Zhang, D. Wang, and J.-G. Zhang, *J. Electrochem. Soc.*, **156**, A773 (2009).
10. T. Shiga, H. Nakano, and H. Imagawa, U.S. Pat. 2008/0299456 A1 (2008).
11. S. S. Zhang, D. Foster, and J. Read, *J. Power Sources*, **195**, 1235 (2010).
12. R. Kou, Q. Hu, D. Wang, V. T. John, Z. Yang, and Y. Lu, *J. Porous Mater.*, **16**, 315 (2009).
13. Y. Meng, D. Gu, F. Q. Zhang, Y. F. Shi, H. F. Yang, Z. Li, C. Z. Yu, B. Tu, and D. Y. Zhao, *Angew. Chem., Int. Ed.*, **44**, 7053 (2005).